Published by :
http://www.ijert.org

International Journal of Engineering Research & Technology (IJERT)
ISSN: 2278-0181
Vol. 10 Issue 06, June-2021

A Compact Two Sleeve Microstrip Patch Rectenna System For Ambient RF Energy Harvesting

Saranya Narayanan[1,*]
Department of ECE
Sri Manakula Vinayagar Engineering College
Puducherry, India

Kesavamurthy Thangavel[2]
Department of ECE
PSG College of Technology
Coimbatore, India

***Abstract*—In this paper, a compact two sleeve microstrip patch rectenna system operated at 2.45 GHz is proposed and implemented for ambient RF energy harvesting applications. The proposed antenna includes microstrip patch and rectangular partial ground plane structure occupies a total area of 26 mm x70 mm, which is simulated and fabricated using a low cost FR-4 substrate with a thickness of 1.6 mm. The two sleeve structures provide compact size and better radiation characteristics. The rectangular slot is introduced at the partial ground plane which improves the bandwidth and impedance matching of the antenna. The measured return loss (S11) better than -10 dB is obtained at the frequency of 2.35 GHz to 2.67 GHz with the fractional bandwidth of 17.14%. The Cockcroft-Walton voltage doubler rectifier circuit with L-type microstrip line impedance matching network is designed and fabricated. The measured results demonstrate that the proposed rectifier circuit achieved the maximum RF to DC conversion efficiency of 45% for 2.45 GHz at the load resistance of 2 KΩ. The DC output voltage of the rectenna is 1.5 V at the input power of +10 dBm.**

Keywords—Rectenna; two sleeve microstrip patch antenna; rectifier circuit; impedance matching network; RF to DC conversion efficiency.

I. INTRODUCTION

In the recent year, self power modern electronic devices have gained significant attentions in a wide range of applications including implantable biomedical devices, automobile devices, battery-free sensors, passive RF Identification (RFID) tags, Internet of Things (IoT) and handheld personal communication equipments [1]. The life time of the battery sources is the most important concern for these devices. The RF energy harvesting is the promising technique that can be used to replace or prolong the life span of the batteries. The concept of RF energy harvesting is to recycling the electromagnetic energy broadcasted from the numerous electromagnetic sources such as cellular towers, Wi-Fi transmitters, TV broadcastings and wireless portable devices. The ambient sources available in the environment are solar, thermal, kinetic, electromagnetic waves etc.

The different methods of energy harvesting from the surrounding sources have been proposed by many researcher. Among the multiple techniques, the method using rectenna technology is much more popular because this method promises enormous scope by providing an alternative green energy solution to many low power electronics devices. The rectenna or rectifying antenna is consists of a receiving antenna, impedance matching network, rectifier circuit, DC pass filter and load resistance, which converts the ambient RF energy into DC power [2]. The power density of the ambient sources available in the environment is very small in the order of microwatt (μW). It is very challenging to harvest the low power density signal with high RF to DC conversion efficiency [3].

Over the last decades, wide varieties of receiving antenna structures and rectifier circuit model have been proposed by many researchers. A dual-band circular patch microstrip antenna with circular slot ground plane structure implemented in [4] has 8.3 and 7.8dBi gain at 1.95 GHz and 2.45 GHz. A multiband four cross dipole rectenna presented in [5] has 41% of conversion efficiency at the incident power of 1.8 mW/ cm^2. Similarly, a microstrip patch array rectenna investigated in [6] has conversion efficiency of 44% at 5.8 GHz. A CPW quad-band rectenna designed in [7] has 42% and 30% conversion efficiency at 0.9 and 2.45 GHz with overall dimension of 48 x 42 mm2. A differentially slot rectenna for RF energy harvesting has been introduced in [8]. The rectenna has 53%, 13% and 15.56% conversion efficiency at 2, 2.5 and 3.5 GHz respectively. A printed monopole antenna fed with CPW ground plane have been investigated in [9]. The rectenna has 45% conversion efficiency at UMTS 2100 band and 33% at GSM 1800 band. Dual band [10-12], multiband [13-15], wideband [16-17] and broadband [18-20] rectenna with the conversion efficiencies of 40%, 30% and 26% are investigated for ambient RF energy harvesting application.

In this work, a compact two sleeve microstrip patch rectenna is presented to harvest the ambient RF energy of 2.45 GHz ISM band. The compact two sleeve microstrip patch antenna with rectifier circuit is proposed having a compact size of 26x70x1.6 mm^3. The microstrip patch structures have several advantages such as low profile, light weight, low fabrication cost and easy mass production in [21-23]. The microstrip patch antennas have some limitations like narrow bandwidth (1 to 5%), low power handling capacity and limited gain. The various techniques have been introduced and developed to overcome the limitations of microstrip patch antenna such as slots on the patch, using low dielectric constant substrate, high substrate thickness and modified ground plane structures. The proposed antenna overcomes the issues presented in the microstrip patch antenna with compact size and better radiation characteristics. A Cockcroft-Walton voltage doubler circuit with simple L-type microstrip

International Journal of Engineering Research & Technology (IJERT)
ISSN: 2278-0181
Vol. 10 Issue 06, June-2021

matching network is designed with maximum RF to DC conversion efficiency. The simulation and experiments are carried out to evaluate the proposed antenna and the rectifier circuit. Finally, the performance of the rectenna is validated by real-time RF energy harvesting testing in an indoor environment.

II. ANTENNA DESIGN

The proposed two sleeve microstrip patch antenna with slot loaded partial ground plane structure front, back and side view configurations are shown in Fig. 1(a, b & c) respectively. The antenna consists of a microstrip patch, two sleeve slots, microstrip feed line and slot loaded partial ground plane. The proposed antenna design started with generic microstrip patch antenna. The long and short sleeve like structures is introduced at the left and right side of the antenna as a result the size of the antenna is reduced without affecting the performance of the antenna. The resonant frequency of the antenna highly depends on the dimensions of long and short sleeves.

The proposed antenna is designed on the FR-4 dielectric material with the dielectric constant of 4.6 and the thickness of 1.6 mm. The compact size is achieved with the help of high dielectric constant material because the aperture area is decreased with increasing the dielectric constant (ε_r). The partial ground plane structure is introduced at the bottom side of the microstrip patch antenna. The partial ground plane technique improves the bandwidth of the antenna. A 50Ω microstrip transmission line is act as a feeding element from which the input power is fed to the antenna. The antenna is fed by a simple insert feeding technique.

The resonant frequency (f_r) of the microstrip patch antenna can be determined from Eq. (1). The resonance frequency of the patch antenna depends on the length of the patch. If the patch length is increases, aperture area, effective dielectric constant (ε_{eff}) and fringing field increases. Hence, the resonance frequency gets decreases and the input impedance plot shifts towards the lower impedance value.

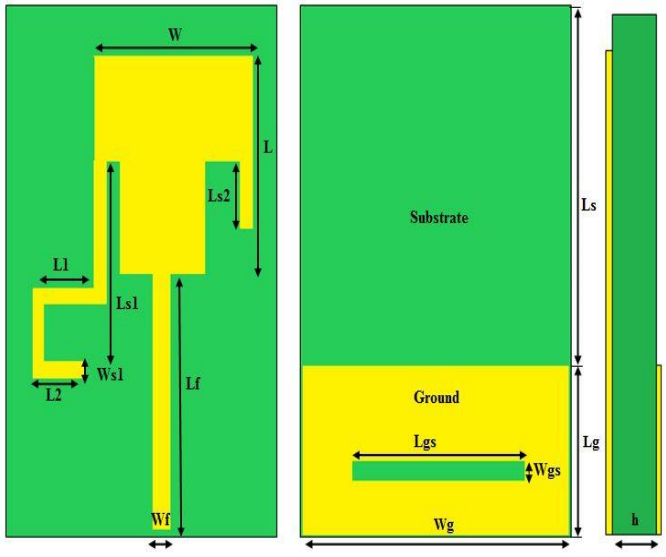

(a) (b) (c)

Fig. 1. Geometry of the proposed antenna (a) Front view (b) Back view (c) Side view.

$$f_r = \frac{C}{2L\sqrt{\varepsilon_{eff}}} \quad (1)$$

where, L is the length of the microstrip patch, C is the speed of the light ($3*10^8$ m/s), ε_{eff} is the effective dielectric constant of the substrate. The width (W) and length (L) of the microstrip patch antenna are calculated using the Eqs. (2)-(3) for the characteristic impedance (Z_0)=50 Ω, dielectric constant (ε_r)= 4.6 and the resonance frequency of 2.45 GHz.

$$W = \frac{1}{2f_r\sqrt{\mu_0+\varepsilon_0}}\sqrt{\frac{2}{\varepsilon_r+1}} = \frac{C}{2f_r}\sqrt{\frac{2}{\varepsilon_r+1}} \quad (2)$$

where, μ_0 is the permeability of the free space ($4\pi \times 10^{-7}$ N/A^2), ε_0 is the permittivity of the free space (8.854×10^{-12} F/m).

$$L = L_e + 2\Delta L \quad (3)$$

where, L_e is the effective length of the antenna and ΔL is the fringing length of the antenna.

$$L_e = \frac{C}{2f_r\sqrt{\varepsilon_{eff}}}$$

$$\varepsilon_{eff} = \frac{\varepsilon_r+1}{2} + \frac{\varepsilon_r-1}{2}\left[1+12\frac{h}{W}\right]^{\frac{-1}{2}}$$

$$\Delta L = 0.412\left\{\frac{(\varepsilon_{eff}+0.30)\left[\frac{W}{h}+0.26\right]}{(\varepsilon_{eff}-0.258)\left[\frac{W}{h}+0.80\right]}\right\}h$$

The width and length of the partial ground plane structure are derived from the finite ground plane condition of the microstrip patch antenna. The width and length of the partial ground plane are calculated from Eqs. (4)-(5). The width of the partial ground plane is the same as the width of the finite ground plane. The length of the partial ground plane is equal to 0.12λ.

$$W_g = 6h + W \quad (4)$$

$$L_g = \frac{\lambda}{8.33} or\ 0.12\lambda \quad (5)$$

In order to improve the return loss (S_{11}) of the antenna, a proper impedance matching between the antenna and the input port is desired. The impedance of the designed antenna is improved by adding the rectangular slot at the partial ground plane structure. The slot is designed at the resonance frequency, which eliminates the imaginary part (reactance) of the antenna. As a result, the impedance matching and return loss of the antenna have been improved [24-26]. To obtain the maximum magnetic coupling in the antenna, the feed line is placed at the right angle to the ground plane slot and the slot is etched at the centre of the ground plane. The slot in the ground plane is placed at the distance of λ/6 or 0.16λ. The width and length of the ground slot are calculated from Eqs. (6)-(7). The calculated dimensions of the proposed antenna are presented in Table 1.

$$L_{gs} = 0.2 \times 5\lambda \quad (6)$$

International Journal of Engineering Research & Technology (IJERT)
ISSN: 2278-0181
Vol. 10 Issue 06, June-2021

$$W_{gs} = 0.1 \times L_{gs} \quad (7)$$

Table 1 Calculated dimensions of the proposed antenna

Parameters	Dimensions(mm)
L_s	34
W	18.1
L	18.05
L_{s1}	24.05
L_{s2}	4.75
W_{s1}	1.1
L_f	3.05
W_f	16.77
W_g	25.4
L_g	11.1
W_{gs}	0.8
L_{gs}	9.4
L_1	4
L_2	3.95

The simulated return loss (S_{11}) of the proposed with and without ground plane slot antennas are compared in Fig. 2(a). The designed antenna without ground plane structure exhibits the return loss of -18.06 dB at 2.434 GHz. The simulated return loss (S_{11}) of the antenna with ground plane slot is -47.733 dB at 2.45 GHz. From the graph it is clear that the return loss of the antenna is improved, when the ground plane slot is introduced at the partial ground plane structure.

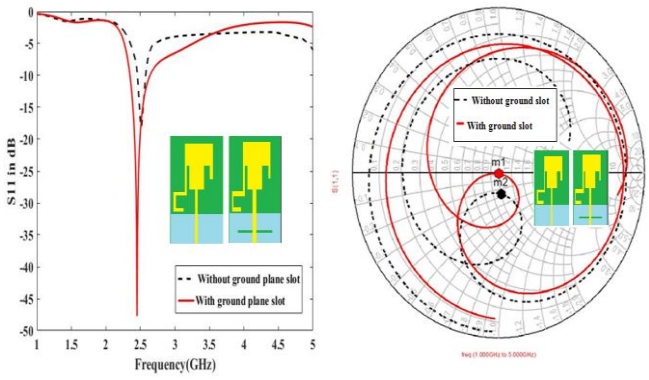

(a) **(b)**

Fig. 2. Comparison of simulated (a) Return loss (S_{11}) (b) VSWR for with and without ground plane slot antenna

Similarly, the comparison of simulated input impedance chart of the proposed with and without ground slot antenna are shown in Fig. 2(b). The simulated input impedance of with and without ground plane structures are Z_{in}=50.4-j0.55Ω and Z_{in}=476.65-j12.05Ω. The impedance of the antenna is perfectly matched with the characteristic impedance of 50 Ω when the ground plane slot is introduced at the partial ground plane. From the above discussion we conclude that the two sleeve microstrip patch antenna with ground plane slot is comparably better in term of return loss VSWR and impedance characteristics.

III. RESULTS AND PARAMETRIC STUDY

In this parametric analysis, four critical parameters of the proposed antenna such as the length of the long sleeve (L_{s1}), length of the short sleeve (L_{s2}), length of the partial ground plane (L_g) and length of the ground plane slot (L_{gs}) have been discussed. The other parameters of the antenna are kept fixed during optimization of the particular parameters. The performance of the antenna is analyzed using the above mentioned parameters.

A. Effect of long sleeve length(L_{s1})

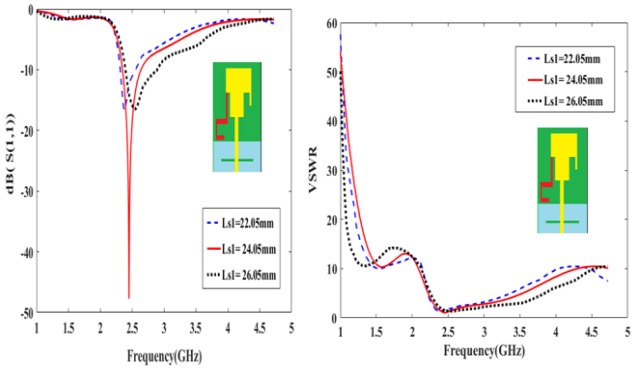

(a) **(b)**

Fig. 3. Simulated (a) Return loss (S_{11}) (b) VSWR for different length of long sleeve (L_{s1}).

The effects of return loss and VSWR versus frequency have been analyzed by varying the length of the long sleeve (L_{s1}). The deviation in the resonant frequency and the return loss (S_{11}) are observed by varying the length of the long sleeve from 22.05 mm to 26.05 mm as seen in Fig. 3(a). The results show that the return loss increases with slight deviation in the resonance frequency. If any change in the resonant length of the long sleeve (L_{s1}), the return loss (S_{11}) increases. The VSWR versus frequency plot for different value of the length is shown in Fig. 3(b). It is concluded that for the optimum value of L_{s1}= 24.05 mm, the return loss (S_{11}) and VSWR of -47.733 dB and 1.008 are achieved at 2.45 GHz.

B. Effect of short sleeve length(L_{s2})

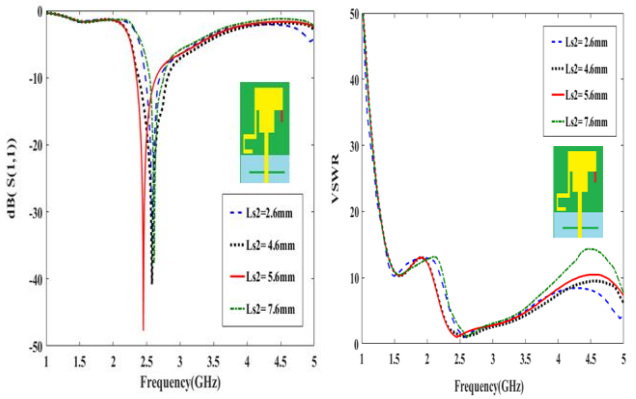

(a) **(b)**

Fig. 4. Simulated (a) Return loss (S_{11}) (b) VSWR for different length short sleeve (L_{s2}).

The effect of return loss and VSWR of the antenna by varying the length of the short sleeve (L_{s2}) are presented in Fig. 4(a) and Fig. 4(b). A slight deviation in the return loss

International Journal of Engineering Research & Technology (IJERT)
ISSN: 2278-0181
Vol. 10 Issue 06, June-2021

with shift in resonance frequency for the different short sleeve lengths 2.6 mm, 4.6 mm, 5.6 mm and 6.6 mm are observed. From the above analysis, the optimum length of the short sleeve should be taken as 5.6 mm, because it gives the minimum return loss of -47.733 dB and VSWR of 1.008 at the resonant frequency of 2.45 GHz.

C. Effect of partial ground plane length(L_g)

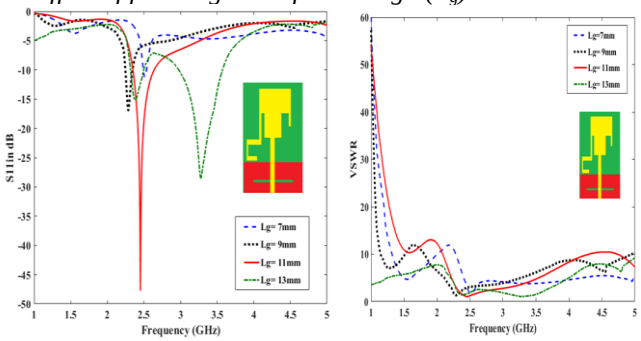

(a) **(b)**

Fig. 5. Simulated (a) Return loss (S_{11}) (b) VSWR for different length of partial ground plane (L_g).

The return loss graph for different partial ground plane length (Lg) is shown in Fig. 5(a). The result shows large deviation in the resonant frequency and the return loss (S_{11}). As the length increases from 7 mm to 13 mm, the resonant frequency is shifted towards higher value. At the optimum value of 11 mm, the proposed antennas resonant at the operating frequency of 2.45 GHz with the minimum return loss (S_{11}) of -47.733 dB. The effect of VSWR versus frequency for different partial ground plane length (L_g) is shown in Fig. 5(b).

D. Effect of ground plane slot length(L_{gs})

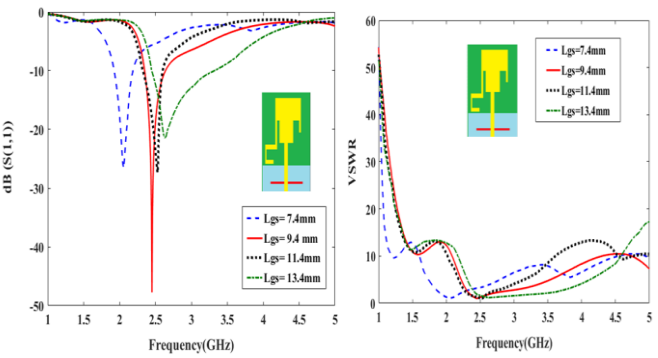

(a) **(b)**

Fig. 6. Simulated (a) Return loss (S_{11}) (b) VSWR for different length of ground plane slot (L_{gs}).

The effect of return loss and VSWR of the antenna at different length of the ground plane slot (L_{gs}) are observed in Fig. 6(a) and Fig. 6(b). By varying the length from 7.4 mm to 13.4 mm, the result shows the deviation in the resonant frequency and return loss. As the length decreases from the resonant length of 9.4 mm, the resonant frequency is shifted to the lower frequency of 2 GHz with the return loss of -28 dB. Similarly, the length is increases from the resonant length of 9.4 mm, the resonant frequency shifted to the higher frequency of 2.8 GHz with the return loss of -20 dB. It is concluded that at the resonant length of 9.4 mm, the antenna exhibits the return loss of -47.733 dB at 2.45 GHz.

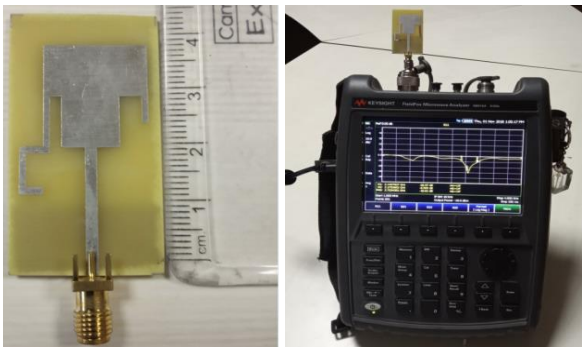

(a) **(b)**

Fig. 7. (a) Fabricated proposed antenna (b) S-parameter measurement test setup.

The fabricated two sleeve microstrip patch with ground plane slot antenna is seen in Fig. 7(a). The S-parameter values are tested with the help of Keysight Vector Network Analyzer (VNA) as shown in Fig. 7(b). The simulated and measured return loss (S_{11}) of the proposed antenna is presented in Fig. 8(a). The simulated and measured return loss (S_{11}) -47.733 dB and -31.60 dB are achieved at the resonant frequency of 2.45 GHz. Fig. 8(b) depicts the simulated and measured VSWR of the antenna. The VSWR of the designed antenna is less than 1.1 at 2.45 GHz. The simulated impedance bandwidth and percentage of fractional bandwidth (% FBW) are 320 MHz (2.35 to 2.67 GHz) and 13.06%. The measured impedance bandwidth and percentage of fractional bandwidth (% FBW) are 420 MHz (2.3 to 2.72 GHz) and 17.14%.

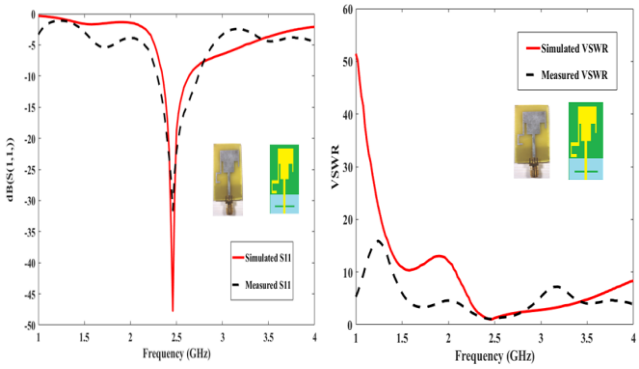

(a) **(b)**

Fig. 8. (a) Simulated and measured (a) Return loss (S_{11}) (b) VSWR of the antenna.

The simulated and measured gain versus frequency plot of the proposed two sleeve microstrip patch antenna with the ground plane slot is presented in Fig. 9(a). The simulated and measured antenna gain of 3.1 dBi and 3 dBi are achieved at the resonant frequency of 2.45 GHz. The simulated surface current density of the proposed antenna with ground plane slot at three different frequencies such as 1 GHz, 2.45 GHz and 5 GHz are shown in Fig. 9(b). At 1 GHz, high current flow only on the feed line of the antenna. Similarly, at 5 GHz the current is distributed evenly in the antenna.

International Journal of Engineering Research & Technology (IJERT)
ISSN: 2278-0181
Vol. 10 Issue 06, June-2021

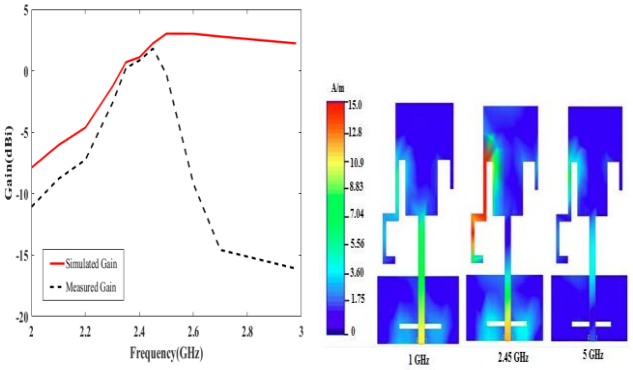

(a) (b)

Fig. 9. (a) Realized gain (b) Current distribution of the antenna

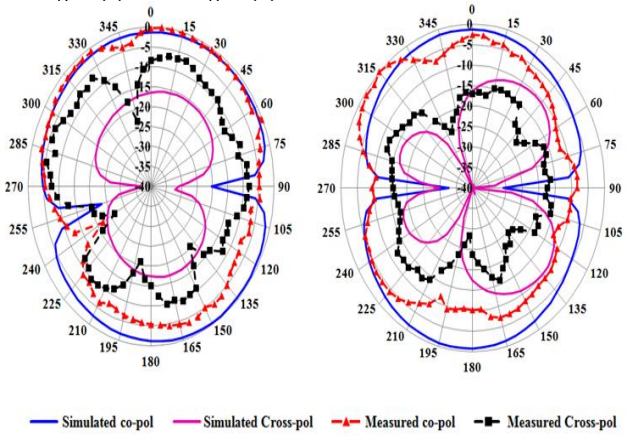

Fig. 9. Simulated and measured far-field radiation patterns at 2.45 GHz (a) E-plane (b) H-plane

At the resonance frequency of 2.45 GHz, the surface current distributed mainly on the sleeves of the antenna, feed line and ground plane slot. These three are the major parameters for the resonance frequency of the proposed antenna. The simulated and measured far-field E and H-plane radiation pattern of the proposed antenna are presented in Fig. 10(a) and Fig. 10(b). It shows that the antenna exhibits low cross-polarization at both E and H-plane of the antenna. It is evident from 2D radiation graph that the antenna performs Omni-directional radiation pattern in E-plane (XZ plane, Φ=0˚) and have almost isotropic radiation pattern in H-plane (YZ plane, Φ=90˚) [27]. The two sleeve microstrip patch antenna with the ground plane slot is suitable for harvesting the ambient RF energy of 2.45 GHz band.

IV. RECTIFIER DESIGN

The rectifier plays an important role in rectenna design because it converts the electromagnetic signal into DC voltage. The block diagram of the proposed rectifier circuit is shown in Fig. 11. The entire rectifier circuit is divided into five main blocks such as input block, impedance matching network, voltage doubler rectifier circuit, DC pass filter and resistive load [28]. The Cockcroft–Walton voltage doubler circuit is used in our design with HSMS-2850 Schottky diode that has ideally low forward bias voltage of 0.15V and fast switching speed at high frequencies which is most suitable for low power RF applications. The topology used for rectifier circuit is presented in Fig. 12(a).

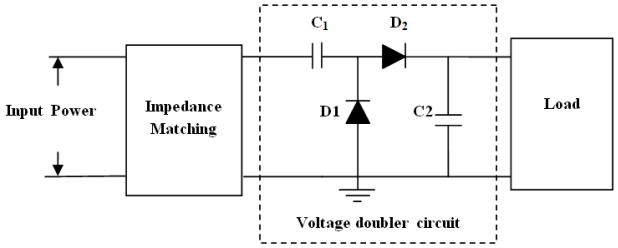

Fig. 11. Block diagram of the proposed rectifier circuit.

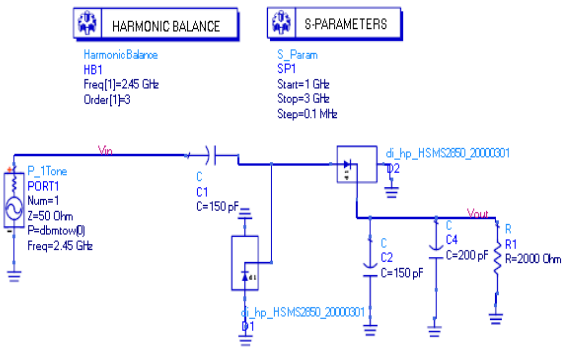

(a)

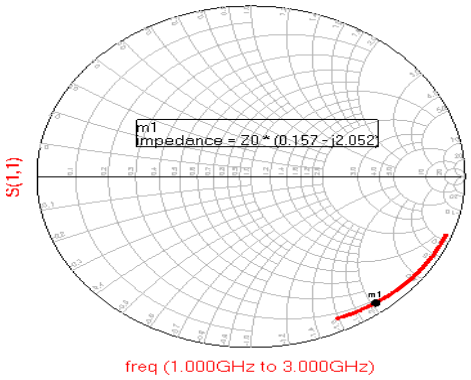

(b)

Fig. 12. (a) Topology of the rectifier circuit (b) Input impedance measurement.

The voltage doubler circuit is made of two Schottky diode D_1 and D_2, charging capacitors C_1 and C_2 and an AC input voltage source. When the input signal is applied to the diode D_1 and D_2 during negative half cycle, the diode D_1 is forward biased and allows the current to flow through the capacitor C_1. The capacitor C_1 is charged to the peak value of the input voltage (V_{ps}). The diode D_2 goes to reverse biased and it does not conduct. In the positive half cycle, the diode D_1 is reverse bias and it does not conduct. The diode D_2 goes to forward biased and it allow the current to flow through the capacitor C_2. At the beginning of the negative half cycle, the capacitor C_2 is discharged, but the capacitor C_1 is charged up to V_{ps}. In the positive half cycle, the capacitor C_2 is charged at twice the input peak voltage ($2V_{ps}$).

International Journal of Engineering Research & Technology (IJERT)
ISSN: 2278-0181
Vol. 10 Issue 06, June-2021

$$C = \frac{Q}{V}$$

$$C = I.\frac{dt}{dv} \quad (8)$$

Here C is the charging capacitors, I is branch current and dt/dv is the ratio of voltage changes with respect to the frequency variation. The charging capacitors C_1 and C_2 value are calculated from Eq. (8). The calculated values of the charging capacitors are C_1 and C_2 is equal to 150pF. The another important block in the rectifier circuit design is DC pass filter which blocks any unrectified AC signal enters into the resistive load. The capacitor (C_{dc}) is act as DC pass filter, whose value is determined from Eq. (9).

$$C_{dc} = \frac{1}{2\pi R_{Load} f_r} \quad (9)$$

Where, R_{Load} is the load resistance of the rectifier circuit. The proposed voltage doubler rectifier circuit is designed by using ADS 2015.01 simulation tool. The simulated input impedance of the rectifier circuit is given in Fig. 12(b). From the plot, the Z_{in} of the voltage doubler circuit is 50*(0.157-j 2.052) Ω. In the rectifier circuit, the receiving antenna is considered as a sources element whose Z_{in} is 50 Ω while the voltage doubler rectifier circuit is considered as a load element whose Z_{in} = 7.85-102.6 Ω.

If these two devices are connected directly as a result the impedance mismatch occurs. An impedance mismatch between the receiving antenna and the rectifier circuit creates the reflected power in the circuit which reduces the efficiency of the system. In these circumstances, the L-type impedance matching network is placed between the antenna and the rectifier circuit which ensures the maximum power transfer between the source and the load. In practice, the inductors are made up of conducting wires of a small area, which may dissipate energy as heat, this leads to degrading of the performances of the rectenna. In order to avoid such constraints, a microstrip line based matching network is used in our proposed rectenna design.

The microstrip line based matching network consists of open and short circuited stubs. The open circuit stub is shunted across the input power source and the short circuited stub connects series with voltage doubler circuit. The impedance of the short circuited stub is calculated from Eq. (10).

$$X_c = Z_0 \cot\theta; \quad \theta < 90^\circ \quad (10)$$

The impedance of the stub is measured from Eq. (11).

$$X_L = Z_0 \sin\theta; \quad \theta < 45^\circ \quad (11)$$

The dimensions of the open and circuited stub are calculated from Eq. (10)-(11). The calculated width and length of the open circuited stub are L_1=15.01 mm and W_1=3.03 mm. The optimized width and length of the short circuited stub are L_2=13.25 mm and W_2=3.03 mm respectively.

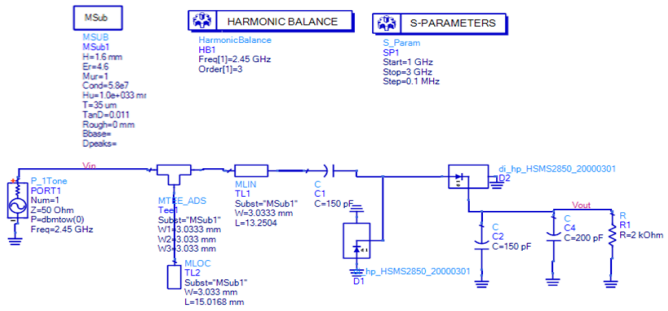

Fig. 13. Schematic diagram of the proposed voltage doubler rectifier with microstrip line matched network.

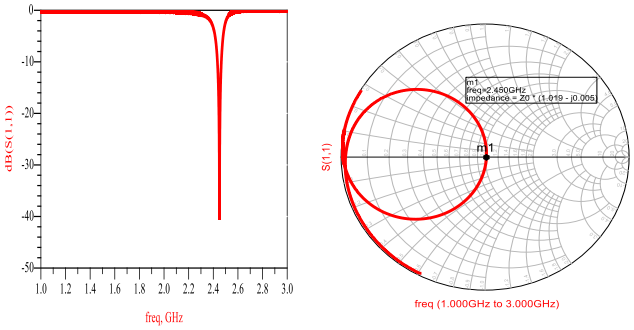

(a) **(b)**

Fig. 14. S-parameter simulation results (a) Return loss (S_{11}) (b) Input impedance (Z_{in}) smith chart.

The microstrip line matching network based voltage doubler rectifier circuit is shown in Fig. 13. The simulated return loss (S_{11}) versus frequency of the proposed microstrip line based voltage doubler circuit is shown in Fig. 14(a). The simulated return loss (S_{11}) of -42 dB is achieved at 2.45 GHz. The simulated input impedance of the rectifier circuit is presented in Fig. 14(b). It shows that the impedance of the rectifier is perfectly matched with the source impedance of 50Ω.

V. RESULTS AND DISCUSSION

The fabricated microstrip line matching network based voltage doubler rectifier circuit S-parameter measurement test setup and measured return loss (S_{11}) plot are shown in Fig. 15(a) and (b). The measured return loss (S_{11}) of -20 dB is achieved at the resonant frequency of 2.45 GHz. The input power of the rectifier is taken from the Keysight Vector Signal Generator (VSG), which generates the input power from -15 dBm to +15 dBm at 2.45 GHz. The input port of the proposed rectifier circuit is directly connected with the signal generator output port. For the different input power value from -15 dBm to +15 dBm, the resulted rectified output voltage and RF to DC conversion efficiency are measured and shown in Fig. 16(a) and Fig. 16(b).

The measured result shows that the proposed rectifier exhibits maximum RF to DC conversion efficiency of 45% at the input power of +10 dBm. The 40% conversion efficiency remains at the input power of +5 dBm to +13 dBm. The measured output voltage of the rectifier is 1.5 V at the input power of +10 dBm. The output voltage range varies from 9 mV to 2.5 V at the input power of -15 dBm to +15 dBm. The proposed antenna and the rectifier circuit are integrated into a single device to form a rectenna. The proposed two sleeve

International Journal of Engineering Research & Technology (IJERT)
ISSN: 2278-0181
Vol. 10 Issue 06, June-2021

microstrip patch rectenna system prototype is presented in Fig. 17(a). In Fig. 17(b) depicts the intentional energy harvesting using signal generator. The proposed rectenna is placed 20 cm away from the transmitter block.

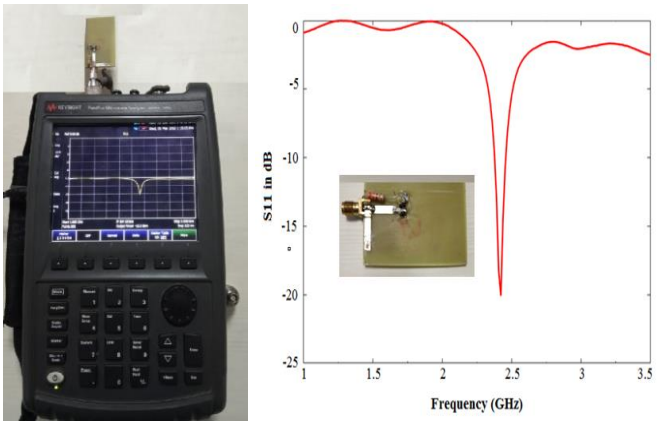

(a) **(b)**

Fig. 15. (a) Fabricated prototype (b) Measured return loss (S11) of the rectifier.

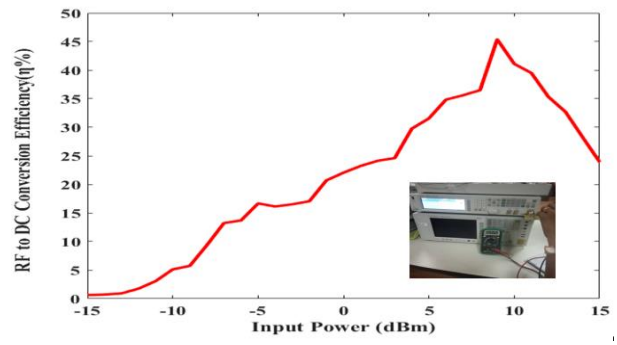

(a)

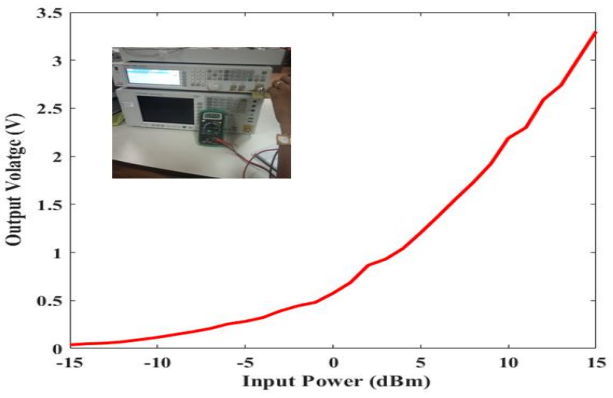

(b)

Fig. 16. Measured (a) RF to DC conversion efficiency (η%) (b) Output voltage (V) vs. Input power (P_{in}) of the proposed rectifier.

The input AC signal with the amplitude of -5 dBm at 2.45 GHz is generated from the signal generator and transmitted via the transmitting antenna. The rectenna receives the incoming signal and converted it into DC voltage with the help of rectifier circuit. The rectified output voltage ranges from 100 mV to 328 mV are achieved. The real-time unintentional RF energy harvesting system as seen in Fig. 17(c). The proposed rectenna receives the Wi-Fi signal from the Wi-Fi system transmitter and rectified it into DC voltage. The rectified voltage ranges from 20 mV to 50 mV at 2.45 GHz ISM band.

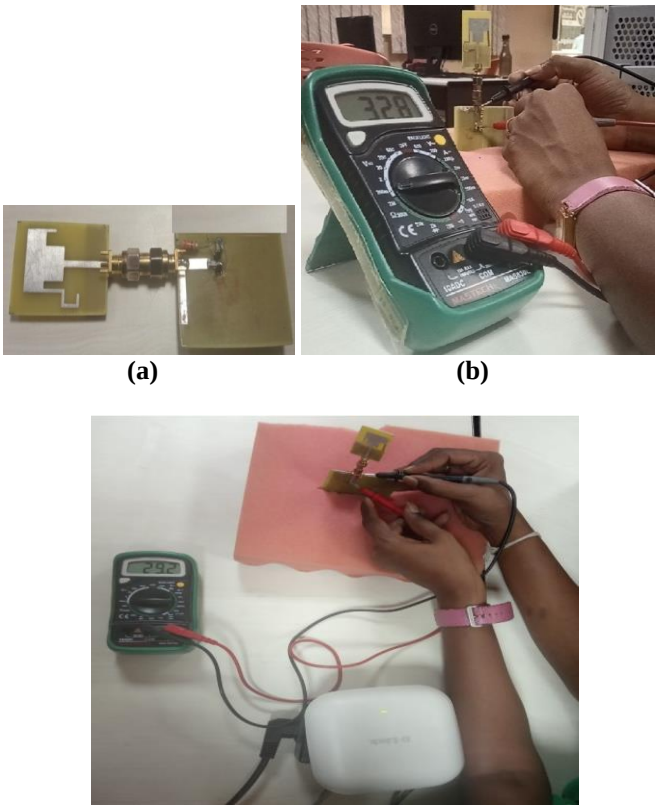

(a) **(b)**

(c)

Fig.17. (a) Complete prototype of the compact rectenna system. (b) Intentional energy harvesting (c) Unintentional energy harvesting.

VI. CONCLUSION

A compact two sleeve microstrip patch along with slot loaded partial ground plane antenna is designed and analyzed. The simulated antenna exhibits the return loss (S_{11}) and VSWR of -47.733 dB and 1.008 at 2.45 GHz. The proposed two sleeve microstrip patch with ground plane slot antenna is fabricated and tested with the help of Vector Network Analyzer (VNA). The measured return loss (S_{11}) of -31.06 dB is achieved at 2.45 GHz with the impedance bandwidth of 420 MHz (2.3 to 2.72 GHz). The measured gain of 3dBi is achieved at 2.45 GHz. The proposed antenna is well suitable for harvesting the ambient RF energy of 2.3 to 2.72 GHz including 2.4 GHz Wi-Fi, 2.45 GHz Bluetooth and 4G (2.5 to 2.7 GHz) bands. The L-type microstrip line matching network based voltage doubler circuit is fabricated and tested. The measured result shows that the proposed rectifier exhibits maximum RF to DC conversion efficiency of 45% at the input power (P_{in}) of +10 dBm. The 40 % conversion remains at the input power (P_{in}) of +5 dBm to +13 dBm. The measured output voltage of the rectifier is 1.5 V at the input power (P_{in}) of +10 dBm. The output voltage range varies from 9 mV to 2.5 V at the input power (P_{in}) of -15 dBm to +15 dBm. The fabricated antenna and the rectifier circuits are integrated to form a rectenna. The rectified output voltage of the rectenna varies from 100 to 328 mV and 20 to 50 mV for intentional and unintentional energy harvesting.

International Journal of Engineering Research & Technology (IJERT)
ISSN: 2278-0181
Vol. 10 Issue 06, June-2021

REFERENCES

[1] Zhou Y, Froppier B, Razban T. Radio frequency ambient level energy harvesting. *Wireless Power Transfer*. 2015; 2(2): 121-126.
[2] Shinohara N. Wireless Power Transfer via Radiawave. John Wiley & Sons: New York; 2013.
[3] Elham K, Alireza H. An ultra-low power, low voltage DC-DC converter circuit for energy harvesting application. *Int J Electron Commun*. 2019; 98: 8-18.
[4] Aboualalaa M, Abdel-Rahman AB, Allam A, Elsadek H, Pokharel RK. Design of a dual-band microstrip antenna with enhanced gain for energy harvesting application. *IEEE Antennas Wirel Propag Lett*. 2017; 16:1622-1626.
[5] Okba A, Takacs A, Aubert H, Charlot S, Calmon PF. Multiband rectenna for microwave applications rectenna multi-bands pour des application micro-ondes. *C. R Physique*. 2017; 18(2):107-117.
[6] Matsunaga T, Nishiyama E, Toyoda I. 5.8 GHz stacked differential rectenna suitable for large-scale rectenna array with DC connection. *IEEE Trans Antenna Propag*. 2015; 63(12): 5944-5949.
[7] Sachine A, Parihar MS, Kondekar PN. A quad-band antenna for multi-band radio frequency energy harvesting circuit. *Int J Electron Commun (AEU)*. 2018; 85: 99-107.
[8] Chandravanshi S, Sarma SS, Akhtar MJ. Design of triple band differential rectenna for RF energy harvesting. *IEEE Trans Antennas Propag*. 2018; 66(6): 2716-2726.
[9] Khemar A, Kocha A, Takhedmit H, Abib G. Design and experiments of a dual-band rectenna for ambient RF energy harvesting urban environment. *IET Microwaves, Antennas Propag*. 2017; 12(1): 49-55.
[10] Sun H, Guo YX, He M, Zhong Z. A dual-band rectenna using broadband Yagi antenna for ambient RF power harvesting. *IEEE Antennas Wirel Propag Lett*. 2013; 12: 918-921.
[11] Shanmuganantham T, Ashok Kumar S. Design of an implantable CPW fed dual dipole antenna for dual band biomedical applications. *Int J Biomed Engg Techno*. 2014; 14: 46-59.
[12] Niotaki K, Kim S, Jeong S, Collado A, Georgiadis A, Tentzeris MM. A compact dual-band rectenna using slot-loaded dual band folded dipole antenna. *IEEE Antennas Wirel Propag Lett*. 2013; 12: 1634-1637.
[13] Palazzi V, Hester J, Bito J, Alimenti F, Kalialakis C, Collado A, Mezzanotte P, Georgiadis A, Roselli L, Tentzris MM. A novel ultra-lightweight multiband rectenna on paper for RF energy harvesting in the next generation LTE bands. *IEEE Trans Microwave Theory and Techniques.* 2018; 66(1): 366-379.
[14] Neeta S, Kanaujia BK, Mirza TB, Mainuddin, Taimoor K, Sachin Kumar. A dual polarized multiband rectenna for RF energy harvesting. *Int J Electron Commun. 2018;* 93:123-031.
[15] Song C, Huang Y, Carter P, Zhou J, Yuan S, Xu Q, Kod M. A novel six-band dual CP rectenna using improved impedance matching technique for ambient RF energy harvesting. *IEEE Trans Antennas Propag*. 2016; 64(7): 3160-3171.
[16] Awais Q, Chattha HT, Jamil M, Jin Y, Tahir FA, Rehman M. A novel dual ultra wideband CPW-fed printed antenna for internet of things (IoT) application. *Journal Wire Commun Mobile Computing*. 2018; 2018: 1-9.
[17] Agrawal S, Ravi DG, Manoj SP, Praveen NK. A wideband high gain dielectric resonator antenna for RF energy harvesting application. *Int J Electron Commun*. 2017; 78: 24-31.
[18] Shi Y, Jing J, Fan Y, Yang L, Li Y, Wang M. A novel compact broadband rectenna for ambient RF energy harvesting. *Int J Electron Commun*. 2017; 95: 264-270.
[19] Song C, Huang Y, Carter P, Zhou J, Joseph SD, Li G. Novel compact and broadband frequency-selectable rectennas for a wide input-power and load impedance range. *IEEE Trans Antennas Propag*. 2018; 66(7): 3306-3316.
[20] Song C, Huang Y, Zhou J, Zhang J, Yuan S, Carter P. A high-efficiency broadband rectenna for ambient wireless energy harvesting. IEEE *Trans Antennas Propag*. 2015; 63(8): 3486-3495.
[21] Palandoken M. Microstrip antenna with compact anti-spiral slot resonator for 2.45 GHz energy harvesting applications. *Microwaves Optical Techno Lett*. 2016; 58(6): 1404-1408.
[22] Shen S, Chiu CY, Murch RD. A dual-port triple-band L-probe microstrip patch rectenna for ambient RF energy harvesting. *IEEE Antennas Wirel Propag Lett*. 2017; 16: 3071-3074.
[23] Taha AE. Novel UWB printed metameterial microstrip antenna based organic substrate for RF energy harvesting applications. *Int J Electron Commun*. 2019; 101: 44-53.
[24] Zhang L, Jiao YC, Song K, Zhang FS. A novel broadband CPW-fed asymmetrical slot antenna. *Microwaves Optical Techno Lett*. 2008; 50(11): 2817-2820.
[25] Alphosos AM, Wong YC, Lau KT. Miniature high gain slot-fed rectangular dielectric resonator antenna for IoT RF energy harvesting. *Int J Electron Commun*. 2018; 85: 39-46.
[26] Jiang LT, Gong SX, Hong T, Jiang W. Broadband CPW–fed slot antenna with circular polarization. *Microwaves Optical Techno Lett*. 2010; 52(9): 2111-2114.
[27] Ashok Kumar S, Shanmuganantham T, Dileepan D. Design and development of CPW fed monopole antenna at 2.45 GHz and 5.5 GHz for wireless applications. *Journal of Alexandria Engineering*. 2017; 56(2): 231-234.
[28] Gaurav S, Rahul P, Prabhakar TV, Vinoy KJ. A tuned rectifier for RF energy harvesting from ambient radiations. *Int J of Electron Commun*. 2013; 67: 564-569.
[29] Hosain MK, Kouzani AZ, Tye SJ, Abulseoud OA, Amiet A, Galehdar A, Kaynak A, Berk M. Development of a compact rectenna for wireless powering of a head-mountable deep brain stimulation device. *IEEE J Translational Engg Health Medicine*. 2014; (2): 285-293.
[30] Hosain MK, Kuzani AZ, Samad MF, Tye SJ. A miniature energy harvesting rectenna for operating a head-mountable deep brain stimulation devices. *IEEE Access*. 2015; 3: 223-234.